JOURNAL OF MATERIALS SCIENCE 29 (1994) 5880–5886

Chromium catalysed silicon nitridation

C. G. COFER, J. A. LEWIS
Department of Materials Science and Engineering, University of Illinois at Urbana-Champaign, Urbana, Illinois, USA, 61801

Silicon powder compacts were fabricated with various amounts of chromium (0–5 at %) deposited onto the surface of the silicon powder by a solution-deposition process. These compacts were heated to several maximum temperatures in the range 1100–1250 °C in a flowing 10% H_2/90% N_2 atmosphere to evaluate the effect of the chromium content on the silicon nitridation. It was observed that silicon compacts containing 5 at % Cr were fully nitrided in approximately 3 h at 1150 °C, while less than 8 % nitridation was achieved for pure-silicon compacts (with 0 at % Cr) compacts under the same conditions. Single-crystal silicon wafers with a 50 nm chromium layer were also nitrided; this provided a planar geometry, which facilitated our study of the catalysis mechanism. The rate-controlling process was shown to be first order, which may be indicative of a nucleation-and-growth mechanism, which is commonly observed for α-silicon-nitride formation. This work demonstrates the feasibility of producing reaction-bonded silicon nitride at low temperatures using chromium catalysis, and it indicates the potential for fabricating fibre-reinforced silicon-nitride composites containing thermally sensitive fibres.

1. Introduction

Reaction-bonded silicon nitride exhibits properties (including high thermal-shock resistance, good strength retention at elevated temperatures, and low creep, erosion and corrosion resistance) which make it well-suited for high-temperature structural applications. Reaction bonding is advantageous for the fabrication of both monolithic and composite structures, such as fibre-reinforced ceramics [1–3]. For example, silicon nitride may be grown from an elemental-silicon powder embedded within a fibre preform to produce a composite structure without residual stresses, since a nearly zero bulk dimensional change is observed during nitridation.

The processing of fibre-reinforced-ceramic-matrix composites presents the challenge of not only achieving a fully reacted and dense matrix but doing so without deleteriously affecting the mechanical properties of the fibres. Most commercially available ceramic fibres are unstable above 1200 °C [4]. In particular, small-diameter polymer-derived fibres which can be woven into fabrics tend to be particularly susceptible to degradation at these elevated processing temperatures. Consequently, the composite-processing route must be designed to minimize exposure to temperatures above 1200 °C.

Several investigations have been carried out to further understand and to improve the kinetics of reaction bonding [5–8]. The effects of various processing parameters (including temperature, particle size and surface area, gas composition, pressure and flow rate) have been examined. Although several empirical models have been proposed to explain the observed kinetic behaviour [9, 10], the simultaneous formation of both the α- and the β-phases serves to complicate this behaviour, and this has generated some disagreement in the literature.

It is well-known that the presence of transition-metal impurities in industrial-grade silicon powders results in accelerated rates of nitridation [11]. Experimental results have demonstrated that p.p.m. (parts per million) levels of iron and other metals accelerate nitridation. Boyer and Moulson demonstrated [12] that the presence of $FeSi_2$ favoured β-Si_3N_4 growth into the liquid eutectic at 1350 °C. However, apart from using ultrafine laser-synthesized silicon [13, 14], complete nitridation of silicon powder has not been achieved at temperatures significantly below 1250 °C. Furthermore, the proposed mechanism of rate enhancement by iron impurities may not adequately explain the catalytic behaviour of other transition metals.

Lin [15] made a survey of the effects of several transition metals on the nitridation of silicon powders and found that, in an acidic environment, chromium additions of several weight per cent were the most effective catalysts. However, for these conditions, a large percentage of the starting silicon powder was volatilized. Furthermore, this study did not address the mechanism by which chromium catalyses silicon nitridation.

In the present work, we studied the influence of chromium on the nitridation of silicon under various reaction conditions. We had two specific objectives. First, we aimed to uniformly distribute a thin layer of the chromium catalyst on the surface of the silicon powders. The powders were compacted and subsequently nitrided to examine the catalytic behaviour.

0022–2461

Secondly, we wanted to develop a fundamental understanding of the mechanism by which chromium serves to catalyse the silicon nitridation. This aim was achieved by nitriding a single-crystal silicon wafer on which a chromium film was deposited. This approach, while simulating the powder nitridation, eliminated the particle size and geometry variables. Depth profiling of the films, in conjunction with kinetic data for the compacts, led to the postulation of a reaction mechanism which was consistent with the observed catalytic behaviour.

2. Experimental procedure

2.1. Sample preparation

2.1.1. Preparation of compacted pellets

High-purity silicon powder (Grade 5d, KemaNord Industrikemi, Ljungaverk, Sweden) was used for all the nitridation experiments. The powders were comminuted with silicon-carbide media in either a ball mill or an attritor mill.

Chromium metal was deposited onto the surface of the as-milled silicon powders in concentrations of 1, 3, and 5 at % by the following procedure. Chromium metal (45 μm in diameter) was first dissolved in 10.8 M HCl. Elemental-silicon powder was dispersed in deionized water using an ultrasonic horn. The dissolved chromium was then added to the silicon solution. The entire solution was heated slowly with stirring. Upon evaporation, chromium was precipitated as a hydrated chloride phase onto the surface of the silicon powder.

The as-prepared powders were dry pressed in a 1 cm diameter die at a pressure of 100 MPa. The samples were pressed to a height of 3.5 mm. They were then vacuum bagged and cold isostatically pressed at 175 MPa.

2.1.2. Preparation of thin-film samples

The use of P-type silicon wafers provided a planar geometry for modelling the surface of the silicon powder. Chromium (99.999%) was radio-frequency (r.f.) sputtered at $0.1\,nm\,s^{-1}$ in a vacuum of 5×10^{-6} torr to a thickness of 50 nm on the surface of the silicon wafers. The wafers were then exposed to the same reaction conditions as the powder compacts. Depth profiling and electron microscopy were subsequently performed on the as-nitrided layers in order to determine the mechanism by which the chromium catalysed the nitridation.

2.2. Nitriding conditions

A reactor system was designed to precisely control and monitor the processing parameters governing the reaction-bonding process. Real-time process control was performed using a Keithley data-acquisition system (Keithley Instruments, Inc., Cleveland, OH) in conjunction with Labtech Notebook data-acquisition software (Laboratory Technologies, Inc., Wilmington, MA). This system enabled simultaneous process control and monitoring of the heating profile, of the mass flow (Tylan General, Carson, CA), both upstream and downstream of the reactor vessel, and of the oxygen concentration. The onset of the reaction was determined by measuring the gas consumed by the reacting specimens. Oxygen contents within the gas atmosphere were monitored with a trace-oxygen analyzer (A-Plus Model, Delta F Corporation, Woburn, MA) downstream from the reaction. This enabled measurement of oxygen concentrations to be made to within $\pm$ 0.2 p.p.m.

A two-loop temperature-control system was used to control the specimen temperature. A type-B (pt-30% Rh/pt-6% Rh) thermocouple was placed directly above the reacting specimens and it was enclosed within a closed-end alumina tube to prevent reaction between the thermocouple and the silicon vapour. The reactor vessel consisted of a Lindberg horizontal-tube furnace (Hevi-Duty Model, Lindberg, Watertown, WI) with a 7.6 cm outer-diameter alumina tube. Flanges were specially designed for the ends of the alumina tube in order to provide an effective seal, thereby minimizing oxygen contamination from the environment.

Nitridation conditions were selected which optimized the reaction kinetics. All the experiments were conducted at atmospheric pressure and with a constant flow rate of $50\,c.c.\,min^{-1}$. The nitridation was performed in a reducing environment consisting of an ultra high-purity premix of 10% hydrogen/90% nitrogen gas. Oxygen levels in the gas stream were maintained below 2 p.p.m. While the heating profile was varied in different experiments, a constant heating rate of $5\,°C\,min^{-1}$ was always maintained until the sample reached the intended reaction temperature.

2.3. Specimen characterization

The particle size, distribution and morphology of the as-received and milled silicon powders were determined using a light-scattering analyser (CAPA700, Horiba Instruments, Inc., Irvine, CA) in conjunction with scanning electron microscopy (SEM). Energy dispersive X-ray spectroscopy (EDS) (TN2010, Tracor Northern, Milwaukee, WI) was used to determine atomic distributions on the surface of the powders. Powder-surface areas were then measured with Brunauer–Emmett–Teller (BET) nitrogen-gas adsorption (ASAP 2400, Micromeritics Instrument Corporation, Norcross, GA) SEM was also used to characterize the microstructural development of specimens exposed to various nitridation conditions. Specimens were prepared by sectioning and polishing to a 1 μm finish using standard metallographic techniques.

X-ray diffraction (XRD) (DmaxII Geiger Flex, Rigaku Corporation, USA) was performed on the specimens after the reaction to determine the relative concentration of each of the phases which were present. The specimens were sliced axially and their interior surfaces were analysed by XRD in order to estimate the weight percentage of the silicon which was nitrided. The procedure and calibration curves of Gazzara and Messier [16] were then used to determine the concentration of Si, α-Si_3N_4 and β-Si_3N_4. Compositional depth profiling was performed on coated powders and wafers using both auger electron

spectroscopy (AES) (PHI 660, Perkin-Elmer, Norwalk, CT) and secondary-ion mass spectrometry (SIMS) (IMS 5f, Cameca, France).

3. Results

3.1. Powder properties; as-received, milled and coated

The median particle diameter as a function of milling time for both the ball-milled and the attritor-milled silicon powders is shown in Fig. 1. Clearly, the attritor milling was more effective in reducing the particle size of these powders. After only 5 h of attritor milling, the median silicon diameter was approximately 0.8 μm whereas 72 h of ball milling was required to achieve this same diameter. The surface area of the as-received powder was 2.1 $m^2 g^{-1}$ (determined by BET nitrogen-gas adsorption). Upon attritor milling for 24 h, the surface area of this powder increased to 15.7 $m^2 g^{-1}$. Upon ball milling for 72 h, however, the powder surface area only increased to 7.1 $m^2 g^{-1}$. The larger surface area of the attritor-milled silicon powders led to an enhanced reactivity during the nitridation (this is discussed in the next section).

SEM revealed that the as-received silicon powder had an irregular morphology, with many particles being larger than 5 μm in diameter. In contrast, the silicon powder which had been attritor milled for 24 h was more equiaxed with a large percentage of submicrometre particles. XRD of the as-milled silicon powder revealed residual SiC contamination from the milling media.

A hydrated chromium-chloride phase, $(Cr(H_2O)_4Cl_2)Cl \cdot 2H_2O$, was observed on the as-coated silicon powders by using XRD [17]. EDS mapping indicated a homogeneous distribution of chromium on the surface of the silicon. Furthermore, AES depth profiling verified the presence of chromium chloride on the surface of these powder samples. Thermogravimetric analysis (TGA) revealed that the phase dehydrated at approximately 100 °C as it decomposed to $CrCl_3$. Upon further heating to 1100 °C in the presence of silicon, the chloride reacted to form $CrSi_2$. Crystalline $CrSi_2$ was observed by XRD when a silicon sample with a 5% chromium content was heated to 1200 °C in an inert Ar atmosphere. In the hydrogen/nitrogen atmosphere, $CrSi_2$ was also detected in these samples, but in much lower levels relative to the silicon-nitride phases.

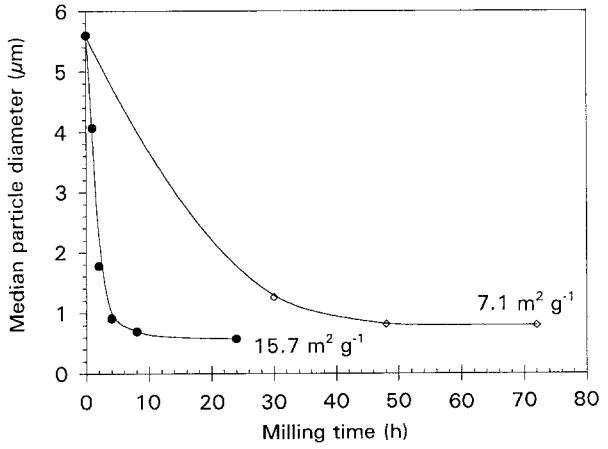

Figure 1 The Median particle diameter as a function of the milling time for: (◇) ball-milled silicon powder, and (●) attritor-milled silicon powder.

3.2. Analysis of the reacted samples

The powder compacts were nitrided for relatively long times of 18 h to provide comparative data on the effects of both the chromium content and the reaction temperature on the nitridation kinetics. Fig. 2a is a three-dimensional plot which illustrates the extent of nitridation as a function of the chromium concentration and the temperature for ball milled (72 h) silicon powder compacts. Other processing parameters (including the reaction time, the pressure, the atmosphere and the flow rate) were held constant for these samples. The percentage nitridation increased significantly as both the temperature and the chromium content increased.

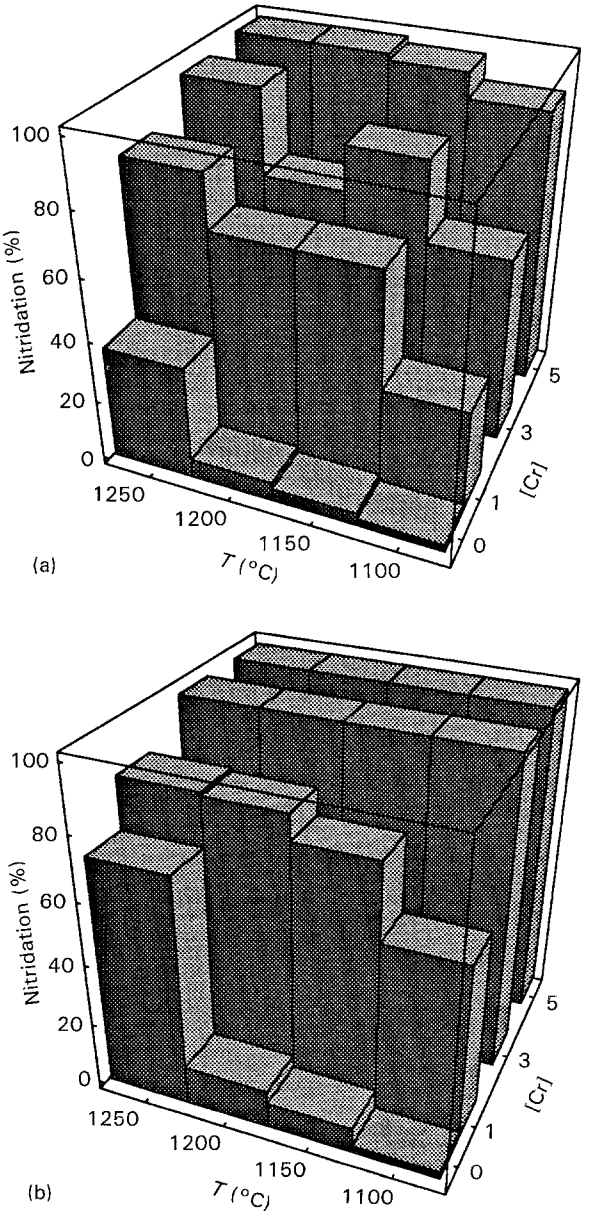

Figure 2 The percentage nitridation as a silicon, function of the reaction temperature and the chromium content for: (a) ball-milled silicon, and (b) attritor-milled silicon.

content increased. For these specimens, the larger surface area of the attritor-milled silicon powder enhanced the nitridation for a given set of conditions. Hence, complete nitridation not only occurred at lower temperatures, but also at lower chromium concentrations. For example, 100% conversion of silicon to silicon nitride was achieved at 1100 °C in specimens with only 3 at % chromium.

In the samples containing chromium, the formation of α-Si_3N_4 was much more prevalent than the formation of β-Si_3N_4 (as determined by XRD). A comparison of the α/β phase ratios as a function of the chromium content for the attritor-milled powders is shown in Fig. 3. It is apparent that the presence of chromium has a dramatic impact on the relative concentrations of α-Si_3N_4 and β-Si_3N_4. While the total weight fraction of the β-Si_3N_4 which formed was relatively insensitive to the chromium content, the amount of α-Si_3N_4 increased dramatically (to as high as 95% of the total weight fraction for the 5 at % Cr specimens). The presence of chromium, therefore, appears to strongly favour formation of the α-phase. This result contrasts sharply with previous results using iron catalysts where β-Si_3N_4 was preferentially formed [12].

A polished cross-section of a specimen with 3 at % Cr which was reacted at 1150°C is shown in Fig. 4. The fine-grained, matted morphology is typical of all of the catalysed specimens, and it is characteristic of α-Si_3N_4 [7]. In contrast, the non-catalysed specimens appeared to be nearly identical to their as-pressed, unnitrided initial condition.

The extent of the reaction was also examined as a function of time for several reaction conditions. These experiments demonstrated that chromium additions increased the reaction rates so that complete nitridation could be achieved in short times at reaction temperatures as low as 1150 °C. In Fig. 5, the percentage nitridation is plotted as a function of the reaction time at 1200 °C for 5 at % Cr and at 1150°C for both 3 and 5 at % Cr. At 1200 °C, complete nitridaton of the 5 at % specimen was achieved within 2 h, while at 1150 °C complete nitridation was achieved within 3 h.

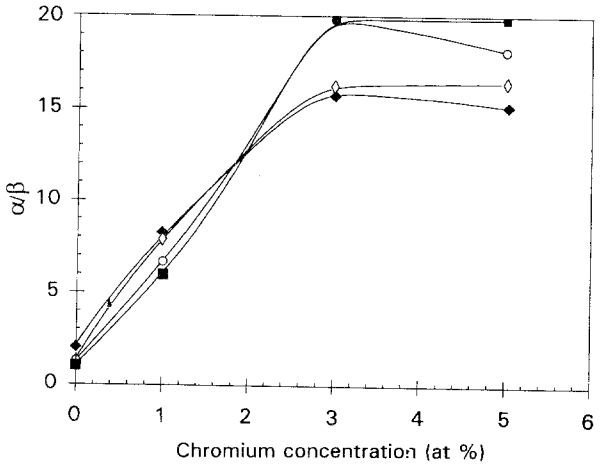

Figure 3 The α/β phase ratio for attritor-milled silicon as a function of the chromium content at various reaction temperatures: (◆) 1250 °C, (◇) 1200 °C, (○) 1150 °C, and (■) 1100 °C.

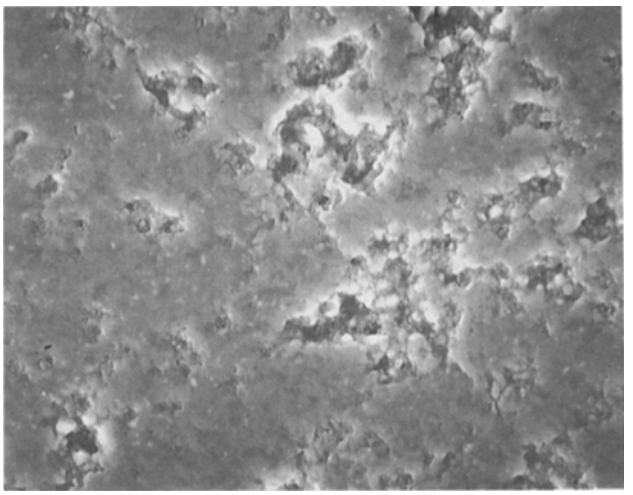

Figure 4 A polished cross-section of a Si/3% Cr pellet which was reacted at 1150 °C.

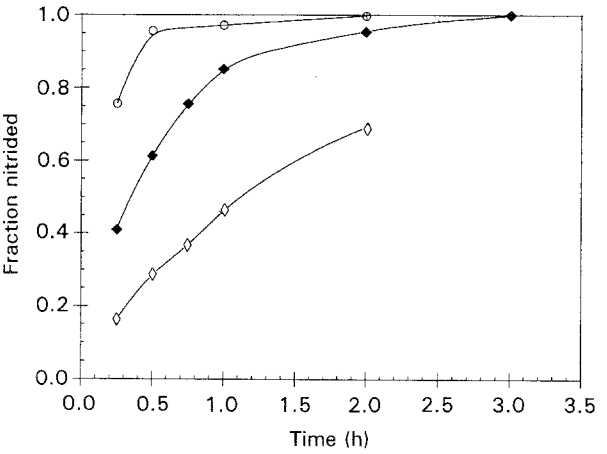

Figure 5 The fraction nitrided as a function of time: (○) 5 at % Cr nitrided at 1200 °C, (◆) 5 at % Cr nitrided at 1150 °C, and (◇) 3 at % Cr nitrided at 1150 °C.

Attritor-milled (24 h) silicon powder compacts with 0, 1, 3 and 5 at % chromium contents were also reacted under the processing conditions described above. The extent of the reaction for these specimens is shown in Fig. 2b. Again, their reactivity was observed to increase as the temperature and the chromium Specimens without chromium additions exhibited less than 8% nitridation under identical reaction conditions.

The kinetic data was further analysed to determine the mechanism of α-Si_3N_4 growth in the presence of chromium. Following previous approaches in the literature [9, 10] the Johnson–Mehl–Avrami equation

$$\phi_\alpha = 1 - \exp(-kt^m)$$

was fit to the fraction of silicon converted to α-Si_3N_4, ϕ_α, at a time, t. This enabled the determination of the reaction parameter, m, which is characteristic of the system geometry. In Fig. 6a, $\ln(-\ln(1-\phi_\alpha))$ is plotted against $\ln(t)$ for specimens with 3 and 5 at % chromium which were reacted at 1150 °C. Linear regression of these curves yielded values of m of 1.00 and 1.22, with correlation factors R, of 0.997 and 0.998, respectively. The data most follows closely the first-

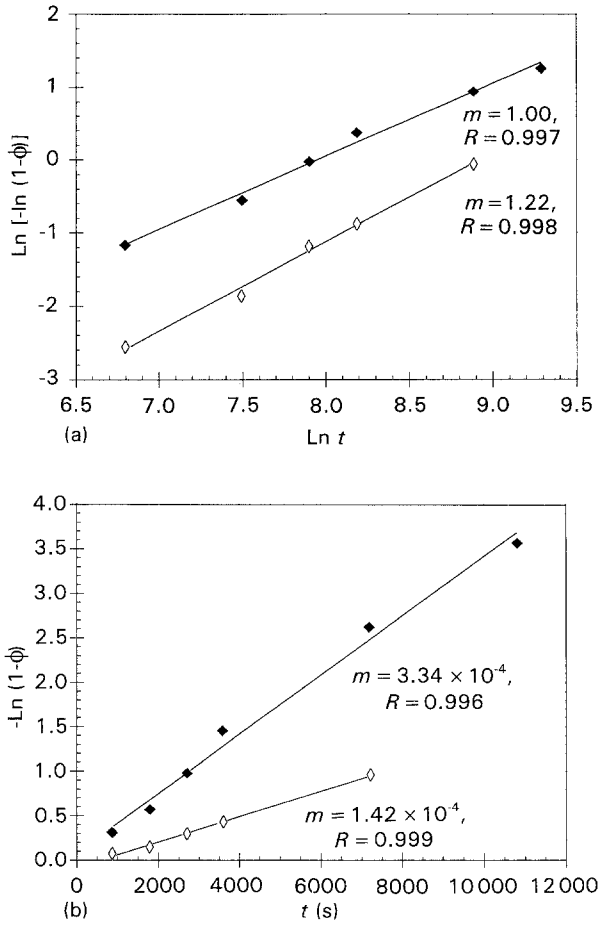

Figure 6 Kinetic data at 1150 °C for determination of: (a) the reaction order, and (b) the reaction-rate constants. (◆) 5 at % Cr, and (◇) 3 at % Cr.

order mechanism.

$$-\ln(1-\phi_\alpha) = k_\alpha t$$

as shown in Fig. 6b. Rewriting this relationship in the form of the power-law model

$$\frac{d\phi_\alpha}{dt} = k_\alpha (1-\phi_\alpha)^n$$

the equation simplifies to the case of n equal to unity for this system. From these curves at 1150 °C, the rate constants were determined as 3.34×10^{-4} and $1.42 \times 10^{-4}\,s^{-1}$, respectively. For solid-state reactions, a first-order kinetic equation suggests that a nucleation-controlled process may be the rate-limiting step [10].

These results are in excellent agreement with the kinetic data of Rahaman and Moulson [18] for α-Si_3N_4 formation on high-purity (oxide-free) silicon powders. Although the reaction temperature (1350 °C) was significantly higher in Moulson's experiment, the kinetic data was also first-order, indicating an identical mechanism for the formation [9, 10]. This conclusion implies that the controlling step in the catalysed system is similar to that in the uncatalysed high-purity-silicon powders. Both systems appear to be controlled by the nucleation and growth of the Si_3N_4 product.

3.3. Silicon-nitride-thin-film growth

In order to investigate the mechanism by which chromium catalyses the formation of silicon nitride, experiments were performed on a model Si system. Chromium metal was deposited on the surface of silicon wafers which were subsequently nitrided. This approach reduced the system to a planar geometry. The characterization was then simplified to one dimension using depth profiling through the thickness of the as-nitrided films to indicate the relative location of the silicon-nitride phase.

AES was used to study the compositional depth profile of the unnitrided wafers. On the unnitrided silicon wafers, the compositional depth profile verified the presence of the 50 nm chromium deposited by r.f. sputtering and showed that a fairly sharp interface existed between this layer and the underlying silicon wafer. AES depth profiles could not be obtained for the as-nitrided Si wafers due to the effects of electrical charging of the nitride phase.

SIMS was used to obtain compositional depth profiles of the nitrided Si wafers and to determine the relative position in which the nitride growth initiated. Fig. 7 illustrates two possible configurations which could result from this process. In the first configuration, the Si_3N_4 grows at the interface between the Si and $CrSi_2$ phases, as shown in Fig. 7a, whereas in the second configuration Si_3N_4 grows on the top surface of the $CrSi_2$, as shown in Fig. 7b. The former configuration is similar to that predicted by previous mechanisms for the Fe catalysis of silicon nitridation described in [12].

Fig. 8 shows the depth profile of a chromium/silicon specimen which was reacted at 1125 °C for 10 min. The results show that a chromium-silicide layer formed as predicted by the Si-powder experiments, and that silicon nitride grew on the top surface of this silicide layer. This profile supports the growth configuration shown in Fig. 7b. Hence, α-Si_3N_4 apparently nucleates at the sites where nitrogen has been adsorbed onto the vapour–solid ($CrSi_2$) interface. In contrast to the Cr-catalysed wafers, specimens of bare silicon exhibited significantly less silicon-nitride growth when they were reacted under the same conditions.

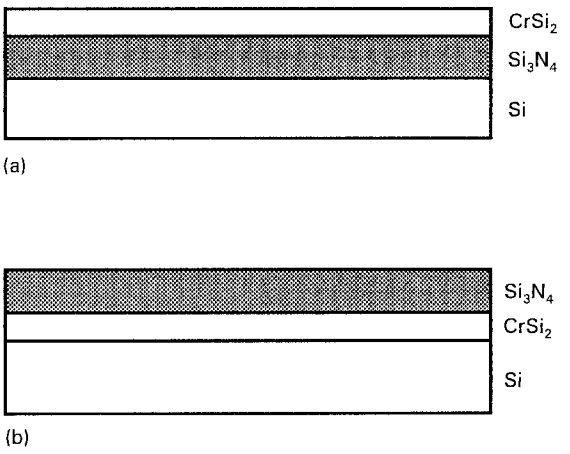

Figure 7 Possible physical configurations for the growth of silicon-nitride films in the presence of a $CrSi_2$ catalytic layer.

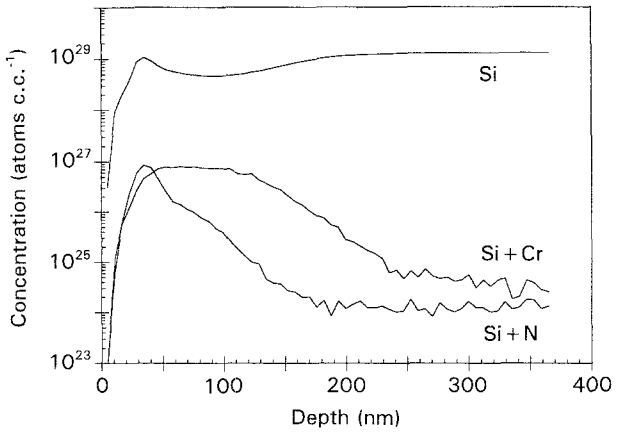

Figure 8 SIMS depth-profile data for a Si/50 nm Cr wafer reacted for 10 min at 1125 °C.

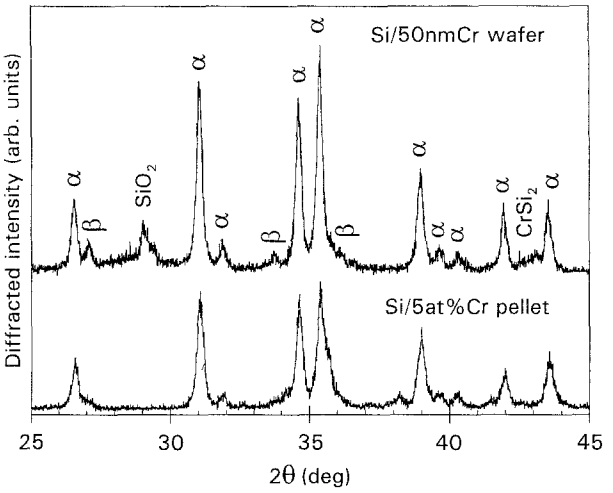

Figure 9 A comparison of XRD diffraction scans of a Si/50 nmCr wafer which was reacted at 1200 °C and a Si/5 at % Cr pellet which was reacted at 1100 °C.

XRD was also performed to verify the validity of the experiment in modelling the powder behaviour. At 1100 °C, prior to the onset of nitridation, $CrSi_2$ peaks were present, indicating reaction of the chromium metal with the underlying silicon. Formation of crystalline α-Si_3N_4 was also observed, demonstrating the same behaviour as was found for the powder compacts.

Longer reaction times resulted in surface roughening as the silicon-nitride growth proceeded on the top surface of the chromium-silicide phase. Nonetheless, the resulting phase composition appeared to be quite similar to those of the pressed silicon/chromium compacts. Fig. 9 shows a comparison between a diffraction scan of a Si/50 nm Cr wafer and a Si/5%Cr pellet, both of which were reacted at 1200 °C for 18 h. In both specimens, α-Si_3N_4 is the dominant phase accompanied by only a slight amount of β-Si_3N_4.

4. Discussion

From the results presented above, a mechanism can be proposed by which chromium catalyses the nitridation of silicon in these experiments. Several observations provide important insight into the physical model.

First, catalysis by chromium was observed at all the temperatures studied (1100–1250 °C), which were well below the lowest chromium-silicide eutectic of 1305 °C. Consequently, the $CrSi_2$ phase remained solid during the thermal processing. In contrast, previous models [12] for Fe-based catalysis were based on the formation of a liquid silicide which accelerated the diffusion and the growth processes.

Secondly, the presence of the chromium catalyst resulted in extensive growth of α-Si_3N_4 relative to the β-Si_3N_4 phase. It has been shown [7] that α-Si_3N_4 grows in the form of a fine matte from the vapour phase, this was also observed in our work (see Fig. 4). In contrast, the addition of other transition metals (for example, Fe) strongly favours the growth of β-Si_3N_4. Therefore, chromium appears to catalyse the nitridation by a completely different mechanism than these impurities.

Finally, analysis of thin-film growth demonstrated that α-Si_3N_4 grew on the top surface of the $CrSi_2$ phase. This indicates that nucleation occurs at sites where nitrogen is chemisorbed. As in other transition metals [20], chromium silicide might be expected to exhibit a very low activation energy for dissociative adsorption of dinitrogen molecules. As the dissociative adsorption should otherwise act as a kinetic barrier, the rate should be accelerated when it is catalysed by chromium silicide.

All of the above observations are self-consistent and they indicate that chromium behaves as a catalyst for silicon nitridation through a mechanism which is distinct from other nitridation catalysts. Formation of the α-Si_3N_4 phase occurs from the vapour phase. Hence, the presence of chromium may act as a catalyst by encouraging chemisorption and subsequent nucleation of this product. As shown schematically in Fig. 10, dissociative chemisorption of nitrogen to the $CrSi_2$ surface is expected. The adsorbed nitrogen species would then react with Si(g), and αSi_3N_4 could subsequently nucleate and grow at the surface. This theory agrees with our kinetic data for the catalysed reaction. As discussed in the analysis of the reacted samples, the time dependence of the reaction follows first-order reaction kinetics and it indicates a mechanism which is controlled by nucleation and growth.

One interesting observation is the dependence of the nitridation rate on the chromium concentration. This is somewhat surprising because less than 1 at % of the catalyst would have been required to provide monolayer coverage on the surface of the powders in the present study. This suggests that the physical mechanism may be more complicated than a monolayer over the surface of the particles. Therefore, the two-dimensional film model is not absolutely conclusive for the powder compacts.

A further complication arises from the presence of the chlorine which is introduced into the gas phase upon the decomposition of the chromium chloride. It is possible that silicon may react with the chlorine thereby forming gaseous $SiCl_4$. Subsequently, the following reaction could occur

$$3SiCl_4(g) + 4NH_3(g) = Si_3N_4(s) + 12HCl(g)$$

$$(\Delta G \approx -128\,kJ\,mol^{-1})$$

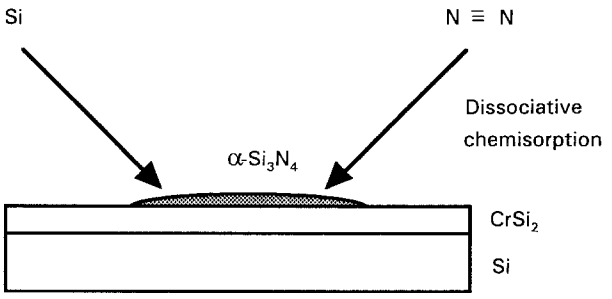

Figure 10 A proposed physical model for the catalysed growth of α-Si_3N_4.

This reaction pathway is one that is commonly used in the chemical vapour deposition of silicon nitride. The reaction is even more favourable when the chromium catalyst is present since the formation of NH and NH_2 radicals are accelerated through the dissociation of N_2. In experiments using HCl with nitrogen in the reacting gas, Si–Cl was observed with a mass spectrometer [15]. While the reaction above may enhance the nitridation rates, the presence of the HCl in the gas phase could have a detrimental effect, resulting in loss of silicon through the gas phase.

While the silicon-nitride product is dominated by the α-Si_3N_4 with the fine matte morphology, it is possible that residual $CrSi_2$ may influence its physical properties. As a grain-boundary phase, the silicide may lower the elastic modulus of the reaction-bonded silicon nitride. Among the silicides, however, $CrSi_2$ exhibits a high oxidation resistance and a rather high melting point of 1550 °C [19]. Its influence on the interfacial characteristics and mechanical properties in fibre-reinforced composites is, as yet, unknown, but it will be a subject of future investigations.

5. Conclusions

The results from the present investigation provide a number of insights into the nitridation of silicon and the extent to which it may be catalysed by chromium.

1. Increasing the silicon surface areas dramatically increases the reactivity with respect to nitridation.
2. A chromium catalyst was effectively deposited from solution as a chloride phase onto the surface of silicon powders.
3. Complete nitridation could be achieved at 1150 °C in 3 h or at 1200 °C in 2 h for attritor-milled silicon powder with 5 at % chromium.
4. The catalysis appears to occur by promoting the dissociative chemisorption of nitrogen followed by silicon-nitride nucleation and growth. This behaviour may be further enhanced by the presence of residual HCL in the atmosphere.

An important consequence of these results lies in the potential for fabricating fibre-reinforced composites using small diameter, thermally sensitive fibres. Through the incorporation of the chromium, the reaction-bonding process can be carried out below 1200 °C, which preserves the integrity of many commercial fibres.

Acknowledgements

The authors would like to thank Aaron Saak for his assistance in collecting data for this work. They would also like to thank ALCOA laboratories for their financial support of this work. The surface analysis was carried out in the Center for Microanalysis of Materials at the University of Illinois, which is supported by the US Department of Energy under contract DEFG02-91-ER45439.

References

1. R. T. BHATT and R. E. PHILLIPS, *J. Compos. Technol. Research* **12** (1990) 13.
2. J. BRANDT, K. RUNDGREN, R. POMPE, H. SWAN, C. O'MEARA, R. LUNDBERG and LARS PEJRYD, *Ceramic. Engng. Sci. Proc.* **13** (1992) 622.
3. T. L. STARR, D. L. MOHR, W. J. LACKEY and J. A. HANIGOFSKY, *ibid.* **14** (1993) 1125.
4. L. M. SHEPPARD (ed), "*Ceramic source*," Vol. 8 (American Ceramic Society, Westerville, OH, 1992).
5. D. MESSIER and W. CROFT, "Silicon Nitride,' *Prep. Prop. Solid State Mater.* **7** (Marcel Dekker, New York, 1982) 131.
6. A. J. MOULSON, *J. Mater. Sci.* **14** (1979) 1017.
7. H. M. JENNINGS and M. H. RICHMAN, *ibid.* **11** (1976) 2087.
8. G. ZIEGLER, J. HEINRICH and G. WÖTTING, *J. Mater. Sci.* **22** (1987) 3041.
9. G. A. ROSSETTI Jr. and R. P. DENKEWICZ Jr., *ibid.* **24** (1989) 3081.
10. A. VARMA, R. G. PIGEON and A. E. MILLER, *ibid.* **26** (1991) 4541.
11. P. POPPER and S. N. RUDDLESON, *Trans. Brit. Ceram. Soc.* **60** (1961) 603.
12. S. BOYER and A. MOULSON *J. Mater. Sci.* **13** (1978) 1637.
13. B. W. SHELDON and J. S. HAGGERTY, *Ceram. Engng. Sci. Proc.* **9** (1988) 1061.
14. *Idem., ibid.* **10** (1989) 784.
15. S. LIN, *J. Amer. Ceram. Soc.* **60** (1977) 78.
16. C. P. GAZZARA and D. R. MESSIER, *Amer. Ceram. Soc. Bull.* **56** (1977) 777.
17. C. G. COFER, "Catalytic nitridation of silicon", M. S. Thesis (University of Illinois at Urbana-Champaign, 1993).
18. M. N. RAHAMAN and A. J. MOULSON *J. Mater. Sci.* **19** (1984) 189.
19. S. P. MURARKA, in "Silicides for VLSI applications" (Academic Press, New York, 1983).
20. J. R. ANDERSON and M. BOUDART, (eds) "*Catalysis science and technology*," Vol. 1 (Springer-Verlag, New York, 1981).

Received 23 September 1993
and accepted 27 May 1994